

APPLICATIONS AND ASSUMPTIONS OF THE API ROD PUMPING DESIGN METHOD - A REVIEW

S. G. Gibbs
Nabla Corporation

ABSTRACT

The American Petroleum Institute (API) method for rod pumping system design became available in the mid 1960's. Even after 30 years, questions still arise concerning its utility. This paper examines basic premises of the API method and how these affect accuracy and applicability. A comparison is made with wave equation techniques which are also widely used. It is concluded that the API method is useful and can be applied with confidence as long as underlying assumptions are not violated.

INTRODUCTION

Development of the API method was not instigated by API. Instead it began in the 1950's as a cooperative effort under the auspices of Sucker Rod Pumping Research, Inc (SRPRI). This non-profit effort was funded by several oil companies and equipment manufacturers. The actual work was done at Midwest Research Institute (MRI) under the direction of the sponsoring companies. An analog computer was constructed to simulate the elastic behavior of the rods as they were driven by a conventional pumping unit. The analog circuits were constructed to simulate anchored tubing and a downhole pump which was filling completely with liquid. The analog computer was capable of creating synthetic dynamometer cards and making predictions of power requirements, unit and rod loadings and pump capacity. Owing to the impracticality of deploying many analog computers for industry use, a graphical method of summarizing the results was developed which became the basis of a hand calculation procedure. At this point, the sponsoring group gave the technology to API (in the early 1960's) and henceforth it has been known as the API method.

A good understanding of the basic assumptions is important. Some of the assumptions are shown in the API literature. Others, less apparent, are included by the writer.

1. Conventional pumping unit motion is presumed.
2. Relatively low slip prime movers are simulated, say equivalent to NEMA D motors and single cylinder gas engines with large flywheel effects.
3. Steel rod strings are presumed. Tapered strings are simulated as if the rods become smaller with depth. Thus large sinker bars on bottom are not handled correctly.
4. Low viscosity fluid friction effects are simulated. Rod drag/tubing drag due to crooked hole or buckled tubing is not considered. Neither is the effect of extreme paraffin deposition.
5. The downhole pump is presumed to fill completely with liquid. Thus the effects of gas interference or fluid pound can not be investigated with the API method. Fluid inertia effects are also not considered.
6. The mechanical predictions are made presuming that the tubing is anchored at the pump.
7. The pumping unit is assumed to be torsionally in-balance.
8. The pumping unit is presumed to have zero structural unbalance.
9. The well is vertical.

As the technical details of the API method were being completed ², the first wave equation solution made its appearance ³. The wave equation combines Newtonian mechanics with Hooke's law of elasticity to simulate the behavior of the sucker rod. The wave equation solution was made feasible by the widespread availability of digital computers. As in the wave equation approach, a good way to understand the API method is in terms of a 'boundary value problem' in mathematical physics. This problem involves solutions to a differential equation (the wave equation in this case) which

satisfy boundary conditions at the top of the rod string (simulation of the prime mover and surface unit) and bottom of the rod string (characterization of the downhole pump). Initial conditions are unimportant inasmuch as steady state behavior is independent of how the system is started. In the following sections, various components of the boundary value problem will be discussed with reference to the API method.

SIMULATION OF THE ROD STRING

After an unfruitful attempt to mimic the rods with a mechanical simulator, an analog computer was devised to solve the equations of motion of a spring - mass- dashpot system such as shown in Figure 1. The motion of a given mass is governed by its own inertia and the downward and upward spring forces acting on it together with the force exerted by the dashpot. The dashpot was included to simulate frictional forces along the rod string. A typical equation of motion (for the 5th mass) is

$$M_5 d^2 Y_5 / dt^2 = k_4 (Y_4 - Y_5) - k_5 (Y_5 - Y_6) - c dY_5 / dt \dots 1$$

In total, nine masses, nine dashpots and eighteen springs were involved which led to nine ordinary differential equations to be solved simultaneously by the analog computer. The simultaneous solution had a coupling effect in which a given mass felt the effects of its neighbors. This approximated the wave propagation behavior exhibited by real, continuous rod strings. Tapered strings were simulated by varying the size of the masses and the stiffness of the springs. In principle, a tapered string could be approximated to the nearest 1/18 th of total length, i. e. the shortest segment could be about 5.5 percent of string length. As equation 1 shows, damping was presumed to be proportional to velocity of the mass as referred to a fixed coordinate system. The damping coefficient was not varied with depth.

As will be demonstrated later, the analog solution has proven very accurate and compares favorably with a wave equation solution.

SIMULATION OF THE SURFACE PUMPING UNIT AND PRIME MOVER

An important boundary condition prescribes how the top of the rod string is driven. This is defined by the motion of the pumping unit as governed by its geometry and the torque versus speed characteristics of the prime mover. Conventional pumping unit motion was chosen. The actual conceptual model was the crank and slider mechanism shown in Figure 2. The model unit lacked a tail bearing, walking beam, saddle bearing and horsehead. Still it mimiced conventional unit motion of the day to a reasonable degree. The surface unit was connected to the rod string by equating the position of the polished rod with the position of the top of the top spring in the rod simulation. H. E. Gray⁴ had shown that average motion for conventional units of the day could be expressed by

$$Y_5 = C \{ \cos \theta + 0.0756 \cos (2 \theta - 174.1^\circ) + 0.0152 \cos (3 \theta - 70^\circ) + 0.0021 \cos (4 \theta + 104.8^\circ) + 0.0005 \cos (5 \theta - 150^\circ) \} \dots 2$$

Inspection of Gray's formula indicated that harmonics higher than the second were small and could be neglected. Workers at MRI showed that motion of the crank/slider mechanism was also dominated by the first and second harmonic components. This led them to select

$$Y_5 = C \{ \cos \theta + 0.06 \cos 2 \theta \} \dots 3$$

as defining conventional unit motion. When equations 2 and 3 are plotted for constant crank velocity, the motions are indeed very similar.

Relatively low slip prime movers were simulated using the linear relationship between motor output torque and speed as shown in Figure 3. Non-linear torque-speed characteristics of real motors were neglected. The defining relationship was

$$T_m = T_o - r \, dV \dots\dots\dots 4$$

T_o was taken to be the average motor torque during a stroke. Motor speed was related to crank angular velocity V through the proportionality factor r which was governed primarily by motor design. As crank speed decreased (negative dV), motor torque output increased and vice versa. The slope of the torque-speed curve was chosen to produce speed variations similar to NEMA D motors.

SIMULATION OF THE DOWNHOLE PUMP

The downhole pump was connected to the rod string by controlling the load on the bottom spring and/or the position of the bottom of the bottom spring. The analog computer was designed to produce a somewhat rectangular downhole pump dynamometer card such as shown in Figure 4. The defining conditions were

$$\text{If } dY_p/dt > 0 \text{ then } F_p = F_o + c_1 \, dY_p/dt \dots\dots 5$$

This implies that as the pump rises (segment b - c), the bottom spring in the simulated rod string is supporting the fluid load and is supplying an additional viscous force associated with lifting fluid up the tubing.

$$\text{If } dY_p/dt < 0 \text{ then } F_p = 0 + c_2 \, dY_p/dt \dots\dots 6$$

The above condition specifies that on the downstroke (segment d - a), the fluid load is borne by anchored tubing and that the lower rod spring is unloaded except for a force which simulates resistance to downward movement due to viscous effects in the pump. It is not clear if viscous effects in the pump were actually included when the graphical design curves were generated.

$$\text{If } 0 < F_p < F_o \text{ then } dY_p/dt = 0 \dots\dots 7$$

Condition 7 prescribes that the pump is stationary at bottom and top of the stroke while fluid load is being transferred to the rods from the tubing or vice versa (segments a - b and c - d).

This type of card occurs when the tubing is anchored at or near the pump, when liquid fillage is complete (no gas interference or fluid pound) and when fluid inertia effects are negligible.

GRAPHICAL DESIGN PROCEDURE

It was impractical to deploy costly and delicate analog computers in many different locations. Instead a graphical design procedure was developed. This involved non-dimensional ratios as follows.

- F_o/Sk_r (non-dimensional rod stretch)
- N/N_o' (non-dimensional pumping speed for tapered rods)
- N/N_o (non-dimensional pumping speed for untapered rods)

Hundreds of runs were made on the analog computer and non-dimensional ratios useful in design were formed. Figure 5 shows typical results obtained with the analog computer. Figure 5-b reveals that the unit was assumed to be in perfect balance. A key presumption was that two distinctly different installations with the same non-dimensional rod stretch and pumping speed would have similar surface and pump dynamometer cards. Certain other ratios would also be the same from well to well such as

- F_1/Sk_r (used to predict maximum rod and structure load)
- F_2/Sk_r (used to predict minimum rod and structure load)
- S_p/S (used to predict pump stroke hence pump capacity)
- $2T/S^2k_r$ (used to predict peak gearbox torque)
- F_3/Sk_r (used to predict polished rod power)

Non-dimensional design graphs were run for one, two, three and four taper rod strings. In the interest of brevity, workers at MRI set out to justify the use of only one set of design curves (a single taper set). Analytical solutions were obtained for a simplified system involving simple harmonic pumping unit motion and zero pump load. A force multiplication factor Q was defined which depicted the ratio of surface dynamic load in a continuous rod string to the dynamic force in a single spring - mass system. Q factors were developed for different pumping speeds and taper designs. Still another factor R was defined which was called the displacement amplification factor. This factor measured the ratio of pump stroke to surface stroke for the simplified system. Similar studies of the simplified system developed natural frequency formulas for various rod tapers. The frequency correction factor F_c was defined such that

$$N_0' = F_c N_0 \dots \dots 8$$

They noted that the values of R for different tapers fell reasonably close to the same line when plotted versus N/N_0' . Similar results were noted for the Q values. This suggested that only one set of 'average' design curves would be sufficiently accurate for practical purposes. Figure 6 shows 'average' graphs plotted in terms of non-dimensional ratios. Paradoxically, most of the final curves were plotted versus N/N_0 instead of N/N_0' , even after the lengthy justification for plotting versus N/N_0' . The writer has located no reason in the surviving record except on page 12-1 of reference 1 where the statement is made "In the analysis of polished rod card area, the best correlation of data was obtained when N/N_0 was used rather than N/N_0' ".

The details of the design calculations will not be presented here. Please consult reference 5 instead.

When the first technical paper appeared which was available to the general public², the implication was given that wave propagation phenomena in the tubing and tubing fluids would be considered. Ultimately, only the dynamic behavior of the rod string was considered as previously described (anchored tubing and rectangular pump cards).

The use of a single set of design curves for all tapers is not perfectly proper. Still the idealization is useful in the API method because only steel strings were treated and sinker bars were not included. Unfortunately, several wave equation programs followed the lead established in the API method wherein the true tapered string is replaced with an untapered string of the same stiffness. When this shortcut is applied to fiberglass-steel strings and sinkerbar designs, predictive accuracy suffers significantly.

Attempts have been made to apply the API method to fiberglass - steel combination strings. These attempts involve replacing the real string with a single taper string of fictitious properties to yield the same stiffness. Unfortunately this causes the predictive method to lose sense of mass distribution (light flexible rods above and heavy stiff rods below). This can cause large predictive errors, particularly in pump capacity.

SPECIFIC APPLICATIONS AND PREDICTIVE ACCURACY

Analysis of rod pumped wells divides naturally into two activities, i.e. 1) design of new installations and 2) diagnosis of existing installations. From the modeling standpoint, the design activity is much more complex than the diagnostic activity. The design model must include simulations of the rod string, the surface unit/prime mover and the downhole pump. The diagnostic activity only involves modeling the rod string. The object of the diagnostic activity is to infer subsurface loads and positions from surface measurements which inherently describe the behavior of the surface unit and prime mover. Thus the matter of simulating surface and subsurface equipment does not even arise. In the discussions

concerning applicability and accuracy of the API method, we shall usually make comparisons with measurements instead of computations. Where required we will use the diagnostic method to draw a conclusion. In rare instances we shall use a wave equation predictive program to illustrate an important finding about the API method.

The workers at MRI did a good job of solving the stated problem. Figure 7 shows the close agreement between analog computer predictions and those made with a digital wave equation program. The case involves simple harmonic pumping unit motion, constant motor speed, single taper rods and a perfectly rectangular downhole pump card. The agreement is remarkable considering that the predictions were made independently and with drastically different methods. Whatever faults inherent in the API method are due to model assumptions, not in deriving results from that model.

Application to Shallow Wells

The API method assumes near constant pump load on the upstroke. This is a good assumption in deeper wells and wells which produce gas. Certain wells, even with anchored tubing and full liquid fillage do not have near constant upstroke pump loads. These wells usually have large pumps set at shallow depths, say 2000 ft or less. They are usually producing mostly water with little free gas. Figure 8 shows such a well where the pump load is not (even) approximately constant as API assumes. The variable upstroke pump load is caused by fluid acceleration and viscous friction effects. The maximum pump load (4040 lbs) is much more than the constant load ($F_0=1250$ lbs) implied by the API model. The variable pump load causes significant predictive errors. In a shallow well, the rods are stiff and impart large accelerations to the fluid which cause additional inertia loads at the pump and departures from the API assumption. In deeper wells the rods are flexible and fluid accelerations are not as large. Free gas in the tubing also tends to diffuse and diminish the fluid acceleration effects. In these cases, the API assumption tends to be borne out. It would be illustrative to predict the behavior of the well shown in Figure 8 using the API method but this is not possible. As probably noted by those who have applied the API method to shallow wells, the nondimensional rod stretch is often out of range of data presented in the design curves. In this case, $F_0/Sk_r = 0.03$ which is below the minimum value studied by API (minimum $F_0/Sk_r = 0.1$). Thus the API method has two difficulties with shallow wells, i.e. 1) well parameters are often out of range and 2) the pump boundary condition used to develop the design data does not fit shallow wells because it neglects inertia.

Certain wave equation programs attempt to mimic fluid acceleration effects. Unfortunately these programs only solve the problem with zero flowline length and constant tubinghead pressure. These conditions rarely occur. The accelerated mass of fluid in the flowline can be a significant portion of the total mass of fluid being pumped. Thus it is improper to neglect the dynamic fluid effects in the flowline. Also, surface check valves can destroy the fluid continuum when intervals under vacuum are formed. At this writing, no satisfactory solution exists which considers dynamic effects in the tubing and flowline fluid columns.

Computation of Fluid Load

The method for computing fluid load in the API methodology needs revision. The pertinent formula (equation 5 in reference 5) is

$$F_0 = 0.34 G D^2 H$$

It can be shown that this formula requires equality of fluid specific gravities in tubing and casing. This is usually untrue since water is continually pumped out of the casing above the pump and gas is usually venting up the casing. A better equation for fluid load which allows for inequality of casing and tubing fluid gravities is

$$F_0 = 0.34 D^2 [G L - G_c Z] \dots\dots\dots 10$$

An example illustrates the point.

D = 2 inch (pump diameter)
 L = 5000 ft (pump depth)
 Z = 2000 ft (submergence over the pump)
 H = L - Z = 3000 ft (net lift)
 G = 1 (specific gravity of tubing fluid)
 G_c = 0.7 (specific gravity of casing fluid above pump)

The API formula suggests

$$F_o = 0.34 (1) (2)^2 3000 = 4080 \text{ lbs}$$

The better formula would suggest

$$F_o = 0.34 (2)^2 [1 (5000) - 0.7 (2000)] = 4896 \text{ lbs.}$$

The example indicates that the API formula tends to underestimate fluid load. Thus actual equipment load would be heavier than anticipated and actual pump capacity would be less than predicted.

Computation of Counterbalance Required

The formula for counterbalance required also needs revision. Following the custom of the day, framers of the API method chose to express counterbalance in terms of effective weight at the polished rod (as contrasted to counterbalance torque). The formula in use was

$$CBE = W_{rf} + 0.5 F_o$$

which implied that ideal effective counterbalance will offset buoyant rod weight plus half of the fluid load. After study, the workers at MRI chose a similar form

$$CBE = 1.06 (W_{rf} + 0.5 F_o) \dots 12$$

which gave good results up to nondimensional speeds of about 0.45. Notably, an unstated assumption was that structure unbalance (B) of the surface unit was zero (neither tail heavy nor horse head heavy). This was approximately true with conventional units of the day. But as stroke lengths were made longer by increasing beam length in front of the saddle bearing, modern conventional units often became horse head heavy (negative structure unbalance). Thus an improved formula of the API type would be

$$CBE = 1.06 (W_{rf} + 0.5 F_o) - B \dots 13$$

An example will help illustrate the point.

$$\begin{aligned}
 W_{rf} &= 8000 \text{ lb}_f \text{ (bouyant weight of rods)} \\
 F_o &= 3500 \text{ lb}_f \text{ (fluid load on pump)} \\
 B &= -1500 \text{ lb}_f \text{ (structure unbalance of horse head heavy unit)}
 \end{aligned}$$

The API formula would specify 10335 lb_f of counterbalance as follows

$$CBE = 1.06 [8000 + 0.5 (3500)] = 10335 \text{ lb}_f$$

The improved formula would specify

$$CBE = 1.06 [8000 + 0.5 (3500)] + 1500 = 11835 \text{ lb}_f$$

Thus the API formula would lead to an under purchase of counterbalance effect. Similarly too much counterbalance effect would be purchased for tail heavy units. Fortunately the established manufacturers of pumping units have realized this shortcoming and routinely account for non-zero structure unbalance.

Effect of Incomplete Pump Fillage on Predictive Accuracy

A key assumption in the API method is that pump liquid fillage is complete. Figure 9 is derived using the diagnostic technique ⁶ and illustrates the errors caused by incomplete liquid fillage. For complete fillage, the predictive accuracy is good (Figure 9-a). When fillage is incomplete (Figure 9-b), larger errors are noted. Usually the peak load is relatively unaffected but gearbox torque is under predicted, polished rod power is over predicted and minimum structure load can err in either direction. The practical conclusion is that the API method should not be applied to wells whose pumps do not fill.

Effect of Fluid Viscosity and Crooked Hole on System Predictions

The design curves were created by the analog computer using relatively low damping values to simulate rod friction. Further the well was presumed to be vertical. Only viscous friction effects between rods and fluid were modeled. The damping value was held constant for each run of the analog computer in the process of generating design data. The actual damping factor used is difficult to determine in hindsight. In the words of the framers 'The best match was found to exist . . . (with damping) being 10 percent of the maximum that could be applied to the analog as installed'. With the help of a wave equation design program, it has been deduced that the damping used was approximately 0.05 as defined in reference 3. Specifically, the API method was used to predict polished rod power for typical values of N/N_0' and F_0/Sk_r . Then the wave equation program was run for the same cases and the damping value of 0.05 was inferred. This is a low value and has been found to apply to near vertical wells with high water cuts and/or gravities in excess of 20 degrees API. Large predictive errors can be expected when viscous producers are analyzed or when crooked holes are encountered. Figure 10-a shows the large predictive errors caused by a viscous emulsion. Figure 10-b shows the large error associated with low viscosity fluid but in a crooked well.

Unit Type Versus Dynamometer Card Shape and Torsional Performance

Unit motion has an important effect on behavior of the rod pumping system because it prescribes the manner in which the rod string is driven. This in turn affects the stress waves that travel in the rod string which control the loads, strokes and dynamometer card shapes that are observed. Pumping unit motion is governed by unit geometry (or type) and characteristics of the prime mover.

There is a fundamental relationship between pumping unit motion and torsional behavior. From energy principles it can be shown for linkage machines that

$$T_f = R(t) / V(t) \dots\dots\dots 15$$

For relatively constant crank velocity $V(t)$, the torque factor T_f varies directly with polished rod velocity $R(t)$. In other words, small torque factors occur with small polished rod velocities and vice versa. This property has been used to advantage in several non-conventional pumping unit designs. Equation 15 then dictates the torque factors and affects dynamometer card shapes which result in a given gearbox load according to the accepted torsional analysis formula ⁷

$$T = T_f (F_s - B) - M \sin (\theta - \tau)$$

Because the API method assumes conventional geometry and because torsional behavior and unit motion are fundamentally linked, the torsional behavior and dynamometer card shape of non-conventional units can not be properly represented by the API technique.

Figure 11-a shows measured surface and computed pump cards derived with the diagnostic technique for a conventional unit. Predictive accuracy is good. Figure 11-b shows the same information for (non-conventional) Mark II geometry for about the same nondimensional parameters. Predictive accuracy is poor with respect to rod loads and torques. Comparison of Figures 11-a and 11-b confirm that unit motion affects dynamometer card shape. Similar results can be shown for other non-conventional geometries. The practical conclusion is that, for best accuracy, the API method should only be applied to conventional units. Errors of varying degrees should be expected when the conventional unit assumption is violated.

System Behavior and Prime Mover Type

At the time the API method was being created, NEMA D motors were the highest slip motors in common use. Later ultra high slip motors came into existence. Probably it is proper to say that API assumed a prime mover much like a modern NEMA D motor. When the API method is applied to ultra high slip motors (and multicylinder engines with small flywheel effects) larger errors should be expected. When prime mover speed varies considerably, the motion of the pumping unit is affected which changes loads, strokes, torques and the shape of the dynamometer card. Larger inertia torques also develop within the drive train. Figure 12-a shows predictions, measurements and diagnostic computations for a NEMA D motor installation. The accuracy is good. Figure 12-b shows the same information for an ultra high slip powered installation with about the same nondimensional ratios. Note that predictive accuracy is not as good and that the larger speed variations have altered the dynamometer card shape. Significant errors in predicted torque are shown. The actual torque has been computed with a method that claims the benefits of inertia⁸.

The analog computer considered drive train inertia effects. Unfortunately no information survives which provides a way to claim the beneficial effects of inertia. The workers at MRI 'arbitrarily adjusted (the analog) to give average inertia as determined by the total speed variation in the cycle'. Thus drive train inertia was used primarily to govern speed variations to levels consistent with NEMA D motors. They did not vary inertia or torque - speed characteristics to simulate the action of ultra high slip motors in various torque modes. Inertia of articulating elements (walking beam, horse head, equalizer beam, etc.) were not modeled but this omission was not serious.

CONTRIBUTIONS OF THE API METHOD IN HISTORICAL PERSPECTIVE

The API Method was developed primarily as a hand calculation technique for designing rod pumping installations. Later a large catalog of tabular results⁹ was created using a digital computer to perform the manual computations. This relieved the user of tedious calculations so that an approximate design could be made quickly. The pre-computed results made it easier to discover the optimum combinations of pump size, pumping speed and stroke length that existed. These were the obvious advancements.

But the API Method made other contributions as well. It was the first to display dynamometer cards in a systematic fashion. Also it demonstrated for the first time the utility of non-dimensional presentation of rod pumping data. In the process of creating design graphs, the analog computer generated synthetic dynamometer cards. These were cataloged¹⁰ versus F_o/Sk_r and N/N_o' . Excerpts from this compilation are shown in Figure 13. When predicted cards are combined with the permissible load concept¹¹, a rational way of selecting pumping parameters to minimize gearbox loading is provided. Even though the API Method only considered conventional geometry, general characteristics like card tilt were revealed for all types of beam units. Conventional units are known to prefer dynamometer cards that slope up-to-right (see for example $F_o/Sk_r = 0.5$ and $N/N_o' = 0.2$ in Figure 13). TorqMaster geometry units prefer cards that are essentially level (see for example $F_o/Sk_r = 0.2$ and $N/N_o' = 0.15$). Mark II and air balanced units are known to prefer down-to-right cards (see for example $F_o/Sk_r = 0.2$ and $N/N_o' = 0.3$). When optimizing gearbox load, it is the designer's task to alter pumping parameters to attain the dynamometer card tilt preferred by the unit to be used. For example a conventional

unit gearbox may be overloaded in a down-to-right condition $F_0/Sk_r = 0.2$ and $N/N_0' = 0.3$. The designer knows to change pumping parameters to move downward and rightward in the array of cards shown in Figure 13. This can be accomplished in various ways by shortening the unit stroke, installing a larger downhole pump or decreasing pumping speed. The card tilt then changes in the direction of up-to-right in keeping with conventional unit preference and hopefully gearbox loads will be reduced. Such understanding would have been more difficult to obtain without systematic presentation of predicted dynamometer cards.

The API Method also impacted diagnostic work in a minor way. When API assumptions are violated, actual dynamometer cards will not appear in collections like Figure 13. When the assumptions are honored, the actual cards will be found in the API results. Knowing the underlying assumptions, the diagnostician can then draw conclusions. For example if an actual card is found in Figure 13, the analyst knows that the pump is filling and that more production is available.

The nondimensional approach has also been useful in correlating wave equation data. In particular, wave equation programs have been used to construct API type non-dimensional graphs for non-conventional geometries¹². Non-dimensional correlations of wave equation data offer an efficient way of making optimization and equipment selection studies.

Many attempts have been made to broaden the applicability of the API method to different unit geometries, prime movers and rod materials. These efforts have not been uniformly successful because the basic data created by the analog computer was based on model assumptions made in the 1950's. The only way to generalize the API method to a new unit geometry would be to construct another analog computer with that unit simulated and repeat the process of creating design data. This is economically impractical in the age of microcomputers whose programs can be easily changed. For best accuracy, the API method should be used in its unaltered state and applied under conditions anticipated by the developers.

SUMMARY AND CONCLUSIONS

1. The API method made significant contributions to the technology of rod pumping. The design computations were conceptually simple. It modeled the most important elements of the rod pumping system and provided predictive accuracy superior to the methods it was intended to replace. A principal contribution was revealing how dynamometer card shape varies with pumping speed and rod stretch. The non-dimensional presentation of design data also was innovative and concise.

2. The API method is still useful for designing rod pumping installations as long as basic assumptions are not violated. Predictive errors of varying degrees should be expected when the assumptions are not honored.

3. The developers of the API method did a good job of solving the stated simulation problem. Any shortcomings are due primarily to basic model assumptions and not to the precision of drawing conclusions from the model.

4. The analog computer approach is no longer the optimum way of creating design data. Digital wave equation solutions are the most feasible and economic avenues at present. Still the analog computer is as capable of solving a rod pumping problem as is a digital computer. The analog is just not as convenient and economic. Some of the concepts used in the API method in presenting data should be employed in future wave equation studies.

NOMENCLATURE

B = structure unbalance of surface unit, $lb_f [N]$

C = surface stroke length factor, ft [m]

c = viscous damping coefficient of i^{th} dashpot in analog simulation of rod string, $lb_f \text{ sec/ft}$
[N sec/m]

CBE = effective counterbalance at polished rod, $lb_f [N]$

c_1 = upstroke viscous coefficient in pump simulation, $lb_f \text{ sec/ft}$ [N sec/m]

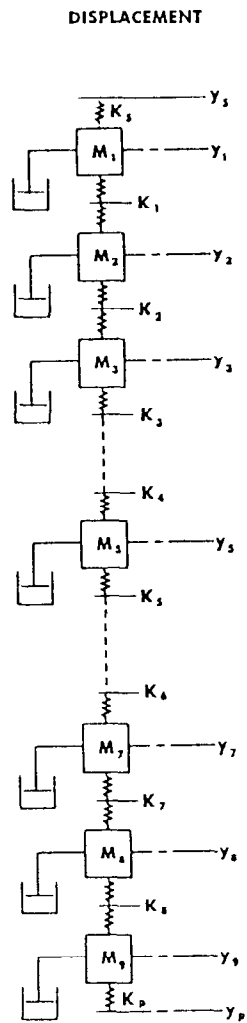
c_2 = downstroke viscous coefficient in pump simulation, $\text{lb}_f \text{ sec/ft}$ [N sec/m]
 D = pump diameter, in [cm]
 F_C = frequency correction factor
 F_0 = fluid load on pump, lb_f [N]
 F_p = downhole pump load, lb_f [N]
 F_1 = peak polished rod load factor, lb_f [N]
 F_2 = minimum polished rod load factor, lb_f [N]
 F_3 = polished rod horsepower factor, lb_f [N]
 F_S = surface rod load, lb_f [N]
 F_X = peak polished rod load, lb_f [N]
 F_n = minimum polished rod load, lb_f [N]
 G = specific gravity of tubing fluid
 G_C = specific gravity of casing fluid over pump
 H = net lift, ft [m]
 k_i = spring constant of i^{th} spring in analog simulation of rod string, lb_f/ft [N/m]
 k_r = total rod string spring constant, lb_f/ft [N/m]
 L = pump depth, ft [m]
 M = maximum counterbalance torque, $\text{lb}_f\text{-in}$ [N-m]
 M_i = mass of i^{th} weight in analog simulation of rod string, lb_m [gm]
 N = pumping speed, cycles/min
 N_0 = natural frequency of untapered rod string, cycles/min
 N_0' = natural frequency of tapered rod string, cycles/min
 P_S = polished rod power, hp [kw]
 r = torque-speed proportionality factor, $\text{lb}_f\text{-ft sec/rad}$ [N-m sec/rad]
 $R(t)$ = polished rod velocity, ft/min [m/min]
 S = surface unit stroke, in [m]
 S_p = downhole pump stroke, in [m]
 T = gearbox torque, $\text{lb}_f\text{-in}$ [N-m]
 T_m = motor output torque, $\text{lb}_f\text{-in}$ [N-m]
 T_0 = average output torque of motor, $\text{lb}_f\text{-in}$ [N-m]
 T_f = torque factor, in [cm]
 T_X = peak gearbox torque, $\text{lb}_f\text{-in}$ [N-m]
 t = time, sec
 $V = V(t)$ = crank velocity, rad/sec
 W_{rf} = weight of rods in fluid, lb_f [N]
 Y_i = position of i^{th} weight in analog simulation of rod string, ft [m]
 Y_p = position of simulated downhole pump, ft [m]
 Y_S = position of polished rod, ft [m]
 Z = pump submergence, ft [m]
 θ = crank angle, rad
 τ = counterbalance phase angle, deg

ACKNOWLEDGEMENT

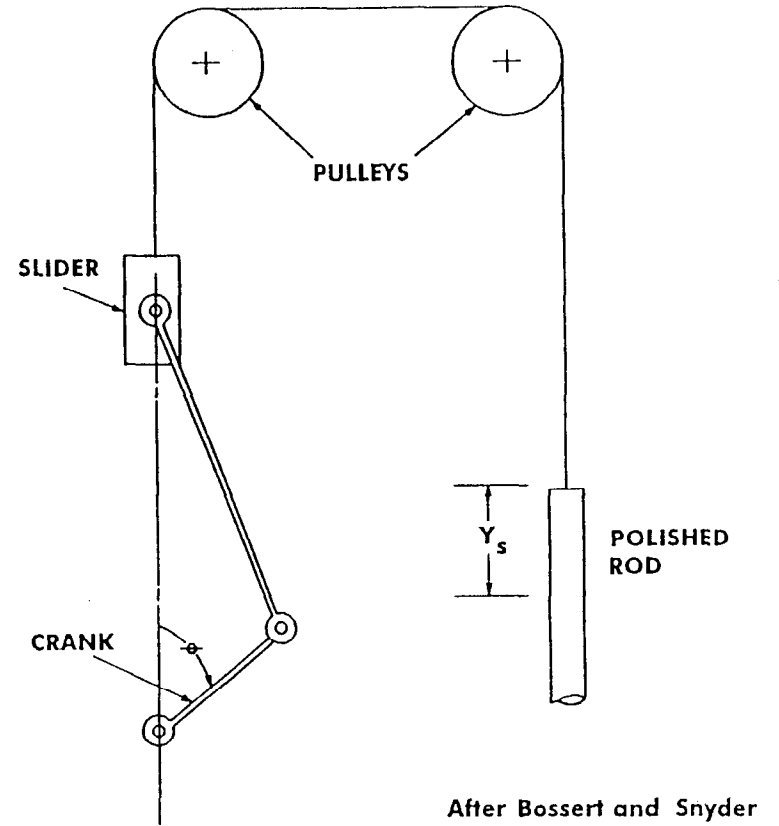
The author thanks Lufkin Industries for loaning an original report concerning development of the API method. This document ¹ has been valuable in comprehending the technical details of the method. The author is also grateful to the University of Tulsa for the opportunity to present a similar paper at their Centennial Petroleum Engineering Symposium.

REFERENCES

1. Bossert, Alfred J. and Snyder, Warren E.: "Study of Sucker Rod Systems," Summary Report Volume I, Midwest Research Institute; Kansas City, Missouri (January 1 - December 31, 1960).
2. Snyder, Warren E. and Bossert, Alfred J.: "Analog Simulation of Sucker Rod Pumping Systems," SPE Paper 587, Presented at the Rocky Mountain Joint Regional Meeting in Denver, Colorado (May 1963).
3. Gibbs, S. G.: "Predicting the Behavior of Sucker-Rod Pumping Systems," JPT (July 1963) 769-78; Trans., AIME, 228.
4. Gray, H. E.: "Kinematics of Oil-Well Pumping Units," API Drilling and Production Practice (1963).
5. American Petroleum Institute: "Recommended Practice for Design Calculations for Sucker Rod Pumping Systems (Conventional Units)"; API RP11L, Fourth Edition; Dallas, Texas (June 1988).
6. Gibbs, S. G. and Neely, A. B.: "Computer Diagnosis of Down-Hole Conditions in Sucker Rod Pumping Wells." JPT (Jan. 1966) 91-98; Trans., AIME, 237.
7. American Petroleum Institute: "Specification for Pumping Units"; API Specification 11E, Sixteenth Edition; Dallas, Texas (October 1989).
8. Gibbs, S. G.: "Computing Gearbox Torque and Motor Loading for Beam Units With Consideration of Inertia Effects." JPT (September 1975).
9. American Petroleum Institute: "Sucker Rod Pumping System Design Book"; API BUL11L3, First Edition; Dallas, Texas (May 1970).
10. American Petroleum Institute: "Analog Computer Dynamometer Cards"; API BUL11L2, First Edition; Dallas, Texas (Dec 1969).
11. Gault, R. H.: "Permissible Load Diagrams for Pumping Units," Presented at 7th Annual West Texas Oil Lifting Short Course, Texas Tech University (April 1960).
12. Clegg, J. D.: "Improved Sucker Rod Pumping Design Calculations," Presented at 35th Annual Southwestern Petroleum Short Course, Texas Tech University (April 1988).



$$M_5 \frac{d^2 Y_5}{dt^2} = K_4 (Y_4 - Y_5) - K_5 (Y_5 - Y_6) - c \frac{dY_5}{dt}$$



$$Y_s = C (\cos \Theta + 0.06 \cos 2\Theta)$$

Figure 1 - Mechanical approximation of rod string

Figure 2 - Simulation of surface pumping unit

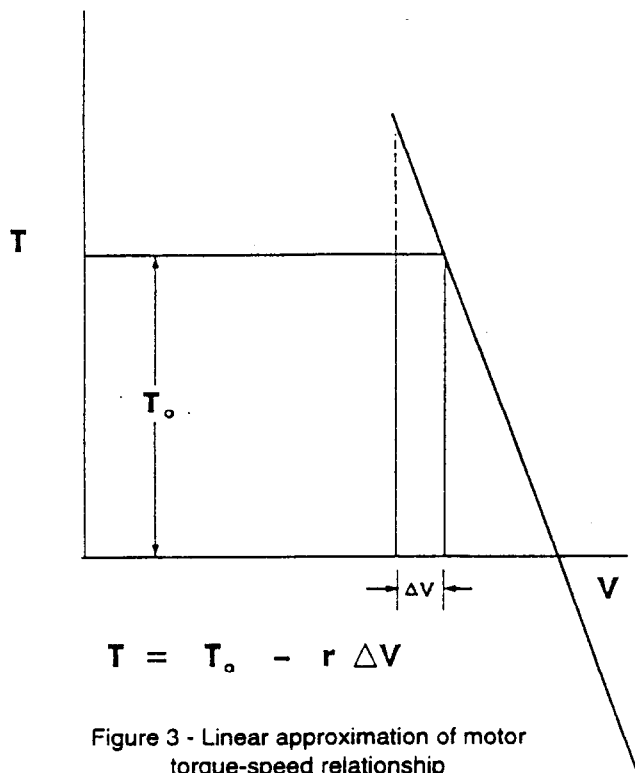


Figure 3 - Linear approximation of motor torque-speed relationship

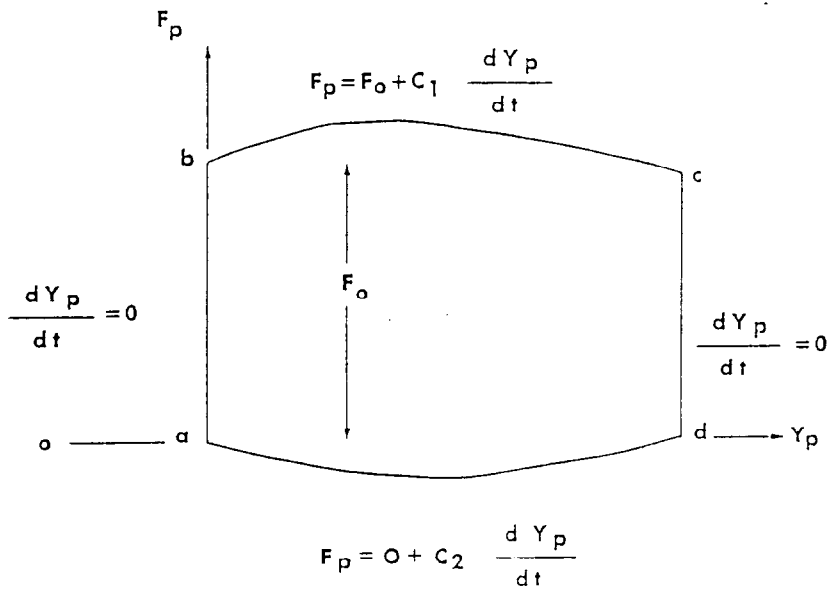
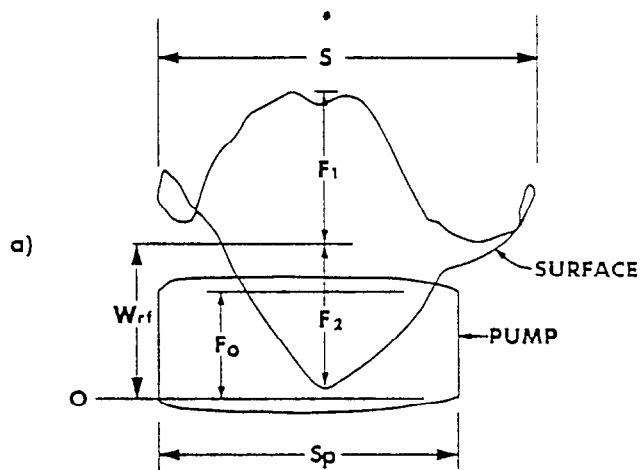


Figure 4 - Simulation of downhole pump assuming full fillage and anchored tubing



After Bossert and Snyder

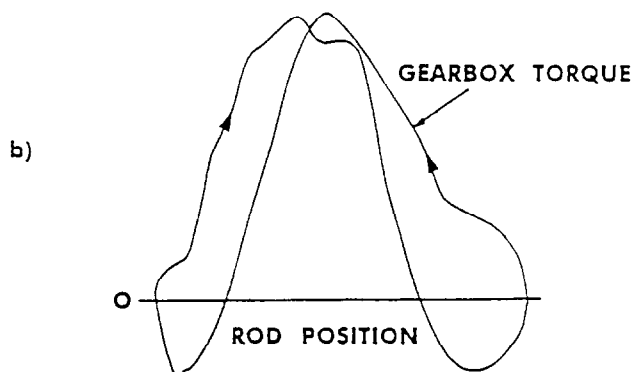
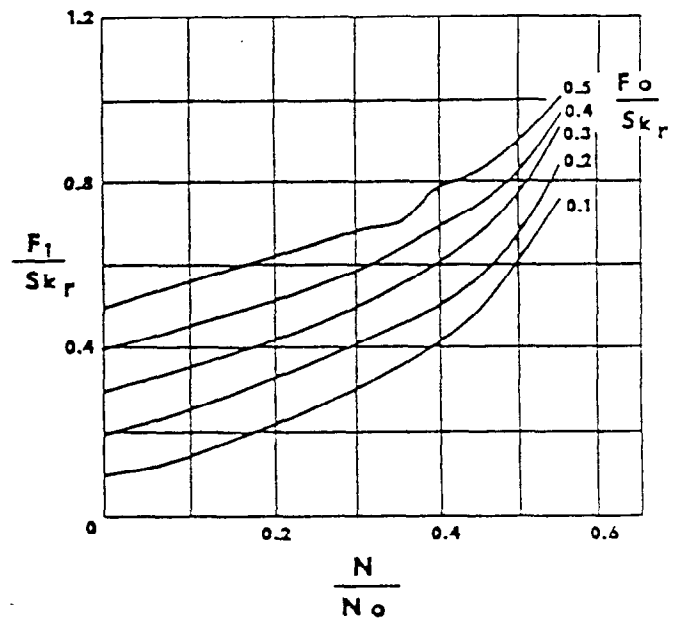
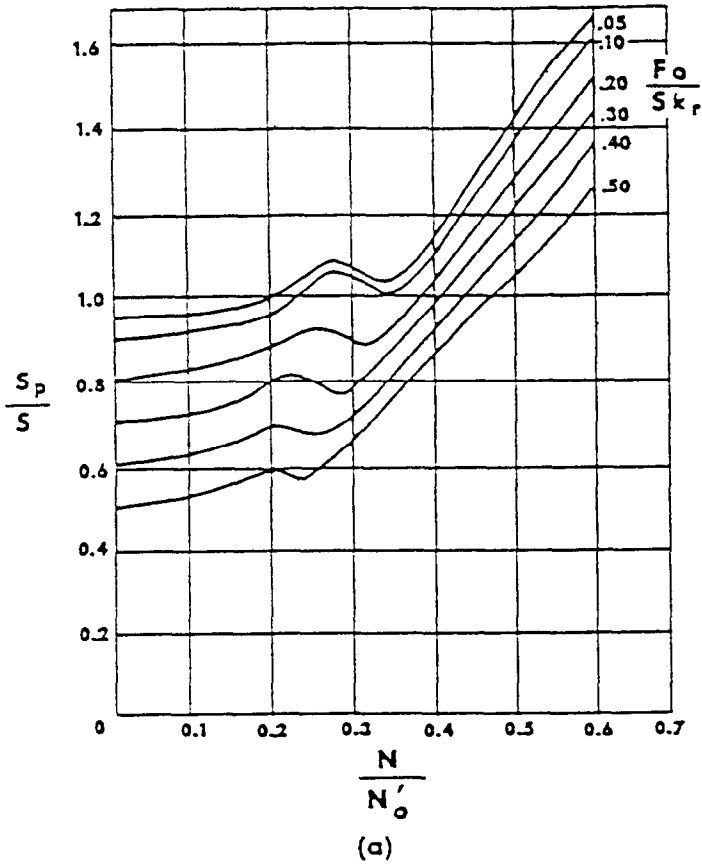
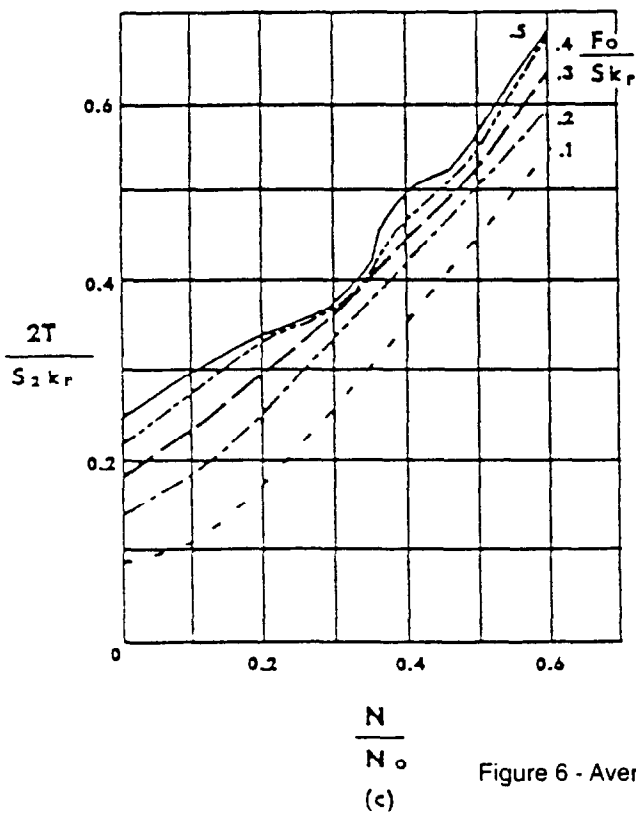


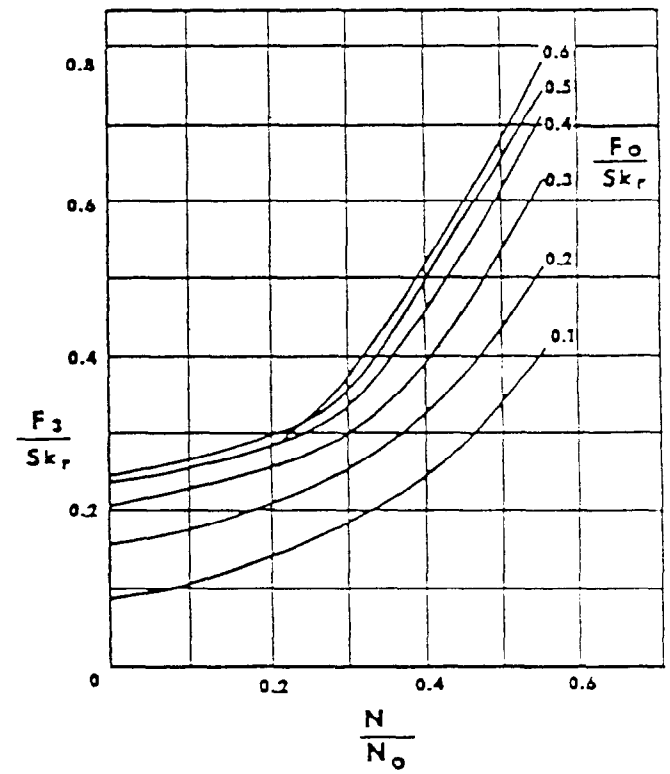
Figure 5 - Typical output from analog computer



(b)



(c)



(d)

Figure 6 - Average nondimensional design graphs

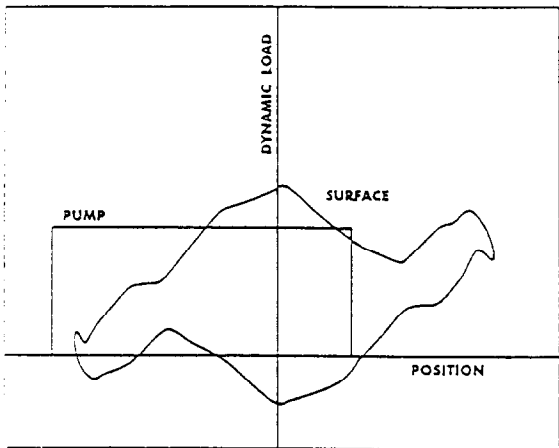
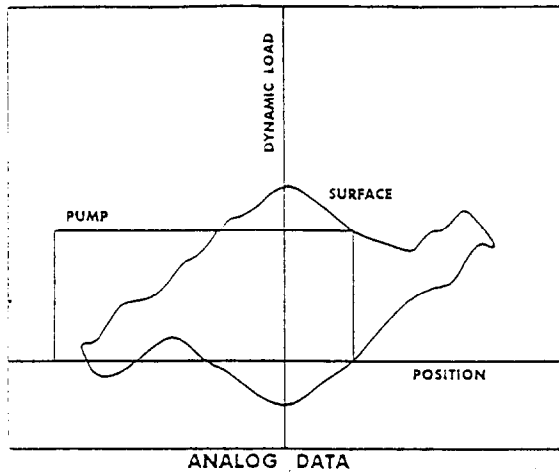


Figure 7 - Comparison of analog and digital computer solutions

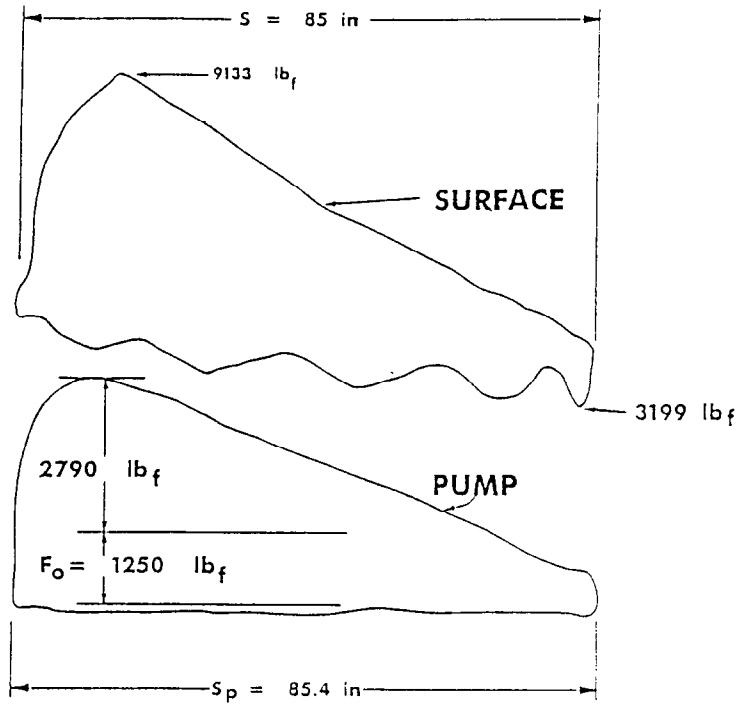


Figure 8 - Surface and pump dynamometer cards showing effects of fluid inertia



$$\frac{N}{N_o} = 0.14 \quad \frac{F_o}{S_{kr}} = 0.13$$

	ACTUAL	PREDICTED	% ERROR
F _x	21856	21230	-2.9
F _n	5979	5870	-1.8
T _x	717.7	687.5	-4.2
S _p	152.3*	151.2	-0.7
P _s	28.9	27.7	-4.2

* COMPUTED WITH DIAGNOSTIC TECHNIQUE

b) PARTIAL FILLAGE



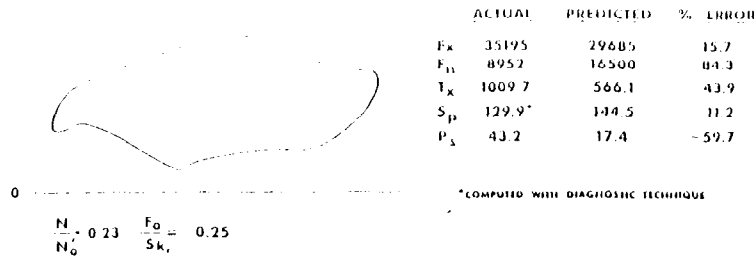
$$\frac{N}{N_o} = 0.14 \quad \frac{F_o}{S_{kr}} = 0.13$$

	ACTUAL	PREDICTED	% ERROR
F _x	21513	21230	-1.3
F _n	3010	5870	95.0
T _x	795.5	687.5	-13.6
S _p	152.7*	151.2	-1.0
P _s	20.8	27.7	33.2

* COMPUTED WITH DIAGNOSTIC TECHNIQUE

Figure 9 - Predictive errors caused by incomplete fillage

a) LOW GRAVITY, EMULSIFIED CRUDE



b) CROOKED HOLE

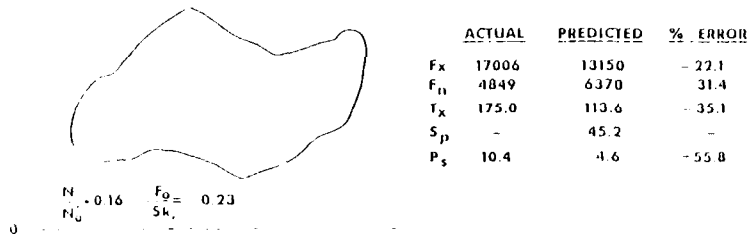
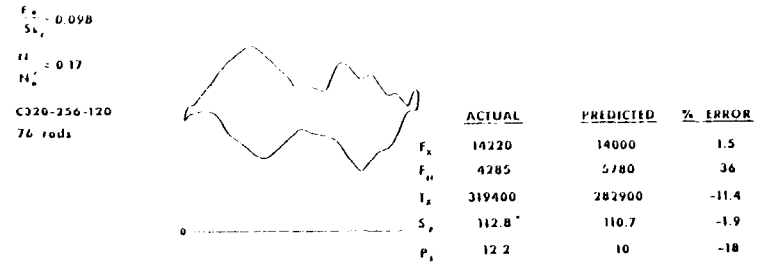


Figure 10 - Effect of excessive downhole friction on predictive accuracy

i) CONVENTIONAL GEOMETRY



j) NON-CONVENTIONAL GEOMETRY

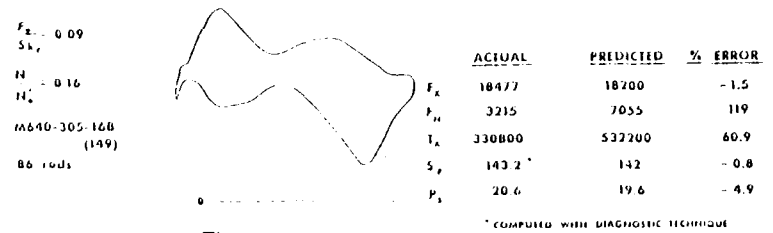
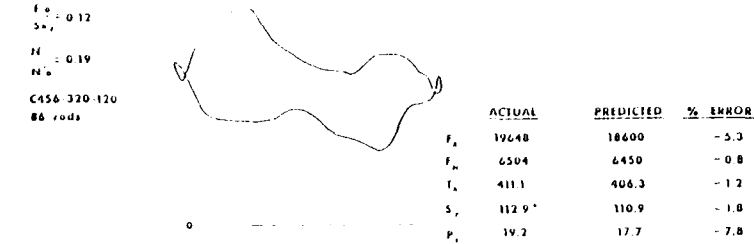


Figure 11 - Effect of unit geometry on dynamometer card shape and design predictions

a) NEMA D MOTOR



b) ULTRA HIGH SLIP MOTOR

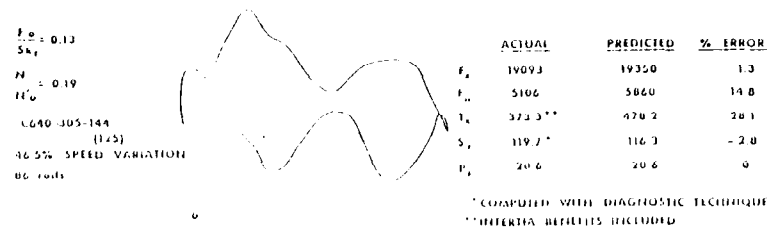


Figure 12 - Accuracy and card shape as affected by motor speed variations

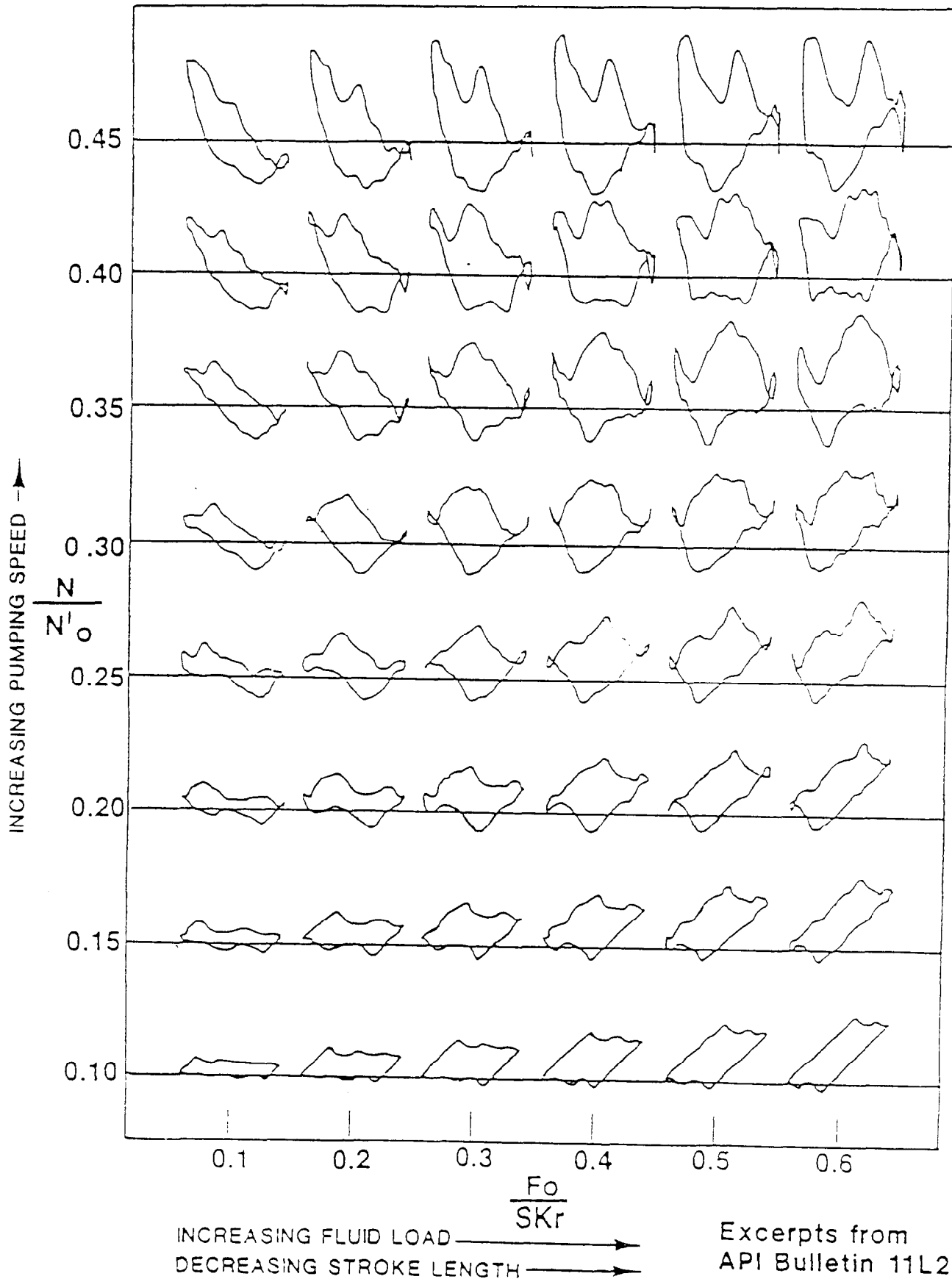


Figure 13 - Synthetic dynamometer cards showing trends in shape and orientation